Supplement of Atmos. Chem. Phys., 25, 13475–13491, 2025
https://doi.org/10.5194/acp-25-13475-2025-supplement

Atmospheric Chemistry and Physics
Open Access
EGU

Supplement of

Potential contribution to secondary aerosols from benzothiazoles in the atmospheric aqueous phase based on oxidation and oligomerization mechanisms

Qun Zhang et al.

Correspondence to: Jianjie Fu (jjfu@rcees.ac.cn)

Section S1. LC-MS analysis conditions for kinetic experiments

Analyses were carried out with a liquid chromatograph (LC, Vanquish, Thermo Scientific, USA) coupled with a triple-quadrupole mass spectrometer (MS, TSQ Altis Plus, Thermo Scientific, USA) equipped with an electrospray ionization (ESI) source. In kinetics experiments with L-phenylalanine (LPA) as the reference compound, analytes were separated using a Thermo Scientific™ Acclaim™ HILIC-1 column (150 mm L × 2.1 mm i.d., 3 µm particle size) at a constant temperature of 40°C. Eluent component A was solution of 40% ultrapure water and 60% methanol containing 10 mM of ammonium acetate. Eluent component B was methanol. An isocratic elution program of 50% A and 50% B was used. In kinetics experiments with suberic acid (SA) and p-Toluic acid (TA) as the reference compound and the products formation experiments, analytes were separated using an Agilent Eclipse column (150 mm L × 4.6 mm i.d., 5 µm particle size) at a constant temperature of 40°C. Eluent component A was 10 mM of ammonium acetate in ultrapure water. Eluent component B was methanol. A gradient elution program was used: 0-1 min 5% B, 1-4 min linear gradient to 95% B, 4-8 min 95% B, 8-9 min linear gradient to 5%B, 9-14 min 5% B.

The ESI conditions were as follows: sheath gas flow rate 50 Arb, aux gas flow rate 15 arb, sweep gas flow rate 0. Collision gas pressure was set to 1.5 mTorr. Nitrogen was used as all four gases listed above. ESI voltage was -2.3 and 3.8 kV in negative and positive modes. The data was acquired only in the multiple reaction monitoring mode (MRM). MRM analysis conditions of analytes are provided in Table S1.

The MS data for each analyte was only acquired in a small time-window, centered around the retention times listed in Table S2 (dynamic MRM method) to enhance selectivity and sensitivity of the analysis. Linearity (dynamic range) of the MS detector was established by analyzing a series of standard solutions with the concentrations between 10 and 150 µM of each analyte. Squared linear regression coefficients (R^2) > 0.995 were obtained for all analytes, thereby confirming a linear relationship between the concentration of the carboxylic acids investigated (independent variable) and the integrated peak areas (dependent variable) under the LC-MS analysis conditions used.

Section S2. LC-Orbitrap MS conditions for chemical composition of organic products

Organic products of the samples were carried out with LC (Vanquish, Thermo Scientific, USA) coupled with the Orbitrap mass spectrometer (Orbitrap Exploris 480, Thermo Scientific, USA) equipped with the ESI probe. Mobile phase A was 10 mM of ammonium acetate in water, and mobile phase B was 100% methanol. 10 μL of samples were injected into a Hypersil Gold C18 column (2.1 mm × 100 mm, 1.9 μm, Thermo Fisher Scientific, USA) and separated with the flow rate of 0.4 mL/min. The spray voltages of ionization were -3.0 and 3.5 kV in negative and positive modes, respectively. The temperatures of ion transfer tube and vaporizer were both 350°C. Sheath gas and auxiliary gas were 35 and 10 arbitrary units (arb).

Table S1. Analysis conditions and fragment ions monitored in the multiple reaction monitoring mode.

Name	Precursor (m/z)	Product (m/z)	Collision Energy (V)	RF Lens (V)
Suberic acid	173	83	18.6	44.1
	173	111	22.2	44.1
	173	154	19.6	44.1
L-phenylalanine	164	72	13.5	49.5
	164	103	16.7	49.5
	164	147	10.3	49.5
p-Toluic acid	135	91	10.3	30.0
benzothiazole	136	65	32.1	76.7
	136	77	24.5	76.7
	136	109	23.8	76.7
2-methylbenzothiazole	150	65	34.5	77.0
	150	69	46.5	77.0
	150	109	23.0	77.0
2-chlorobenzothiazole	170	109	27.3	76.5
	170	134	23.6	76.5
	170	135	24.1	76.5

Table S2. Kinetics data for BT, MBT, and CBT + OH reactions.

Reactant	pH	Reference	$[BTs]_0$:$[Refs]_0$	k_{BTs}/k_{Ref}	R^2	k ($\times 10^9$ M^{-1} s^{-1})
BT	2	SA	1:1	1.97 ± 0.03	0.998	8.0 ± 1.8
			1:2	1.87 ± 0.03	0.998	
			2:1	1.96 ± 0.02	0.999	
		LPA	1:1	1.09 ± 0.03	0.992	
			1:2	1.26 ± 0.03	0.994	
			2:1	1.19 ± 0.02	0.997	
	10	TA	1:1	1.06 ± 0.02	0.996	9.7 ± 2.7
			1:2	0.99 ± 0.02	0.995	
			2:1	1.05 ± 0.03	0.993	
		LPA	1:1	1.08 ± 0.02	0.996	
			1:2	1.32 ± 0.03	0.996	
			2:1	1.29 ± 0.04	0.992	
MBT	2	SA	1:1	1.69 ± 0.03	0.997	7.6 ± 1.7
			1:2	1.68 ± 0.03	0.998	
			2:1	1.62 ± 0.03	0.997	
		LPA	1:1	1.08 ± 0.02	0.998	
			1:2	1.46 ± 0.03	0.997	
			2:1	1.25 ± 0.02	0.997	
	10	TA	1:1	1.23 ± 0.04	0.993	9.8 ± 2.7
			1:2	1.10 ± 0.03	0.994	
			2:1	1.04 ± 0.04	0.991	
		LPA	1:1	1.34 ± 0.04	0.994	
			1:2	1.05 ± 0.02	0.996	
			2:1	1.14 ± 0.02	0.997	
CBT	2	SA	1:1	1.65 ± 0.05	0.990	7.6 ± 1.9
			1:2	1.74 ± 0.05	0.995	
			2:1	2.09 ± 0.07	0.992	
		LPA	1:1	1.11 ± 0.02	0.997	
			1:2	1.18 ± 0.03	0.994	
			2:1	1.08 ± 0.03	0.994	
	10	TA	1:1	0.82 ± 0.02	0.995	9.4 ± 2.7
			1:2	1.18 ± 0.04	0.993	
			2:1	0.98 ± 0.02	0.997	
		LPA	1:1	1.16 ± 0.03	0.995	
			1:2	1.12 ± 0.03	0.994	
			2:1	1.33 ± 0.04	0.992	

Table S3. The molar yield (%) of inorganic products of 5 hours of photooxidation of BT, MBT, and CBT with OH radicals at initial pH 2 and 10.

System	SO_4^{2-}	NO_3^-	Cl^-
BT-pH2	29.5	6.7	-
BT-pH10	30.4	10.1	-
MBT-pH2	46.6	0.1	-
MBT-pH10	41.6	0.2	-
CBT-pH2	25.3	1.9	87.1
CBT-pH10	19.4	0.9	61.5

Table S4. Proposed monomers with the BT moiety from the BT-pH2 experiment analyzed by LC-Orbitrap MS.

Retention time (min)	Ion mode	m/z	Calc. MW	Formula	Proposed structure
5.17	$[M-H]^-$	150.00207	151.00935	C_7H_5NOS	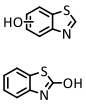
5.65	$[M-H]^-$	150.00202	151.00930		
5.16	$[M+H]^+$	152.01637	151.00909		
5.27	$[M+H]^+$	152.01633	151.00905		
5.48	$[M+H]^+$	152.01631	151.00904		
4.91	$[M-H]^-$	165.99690	167.00418	$C_7H_5NO_2S$	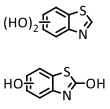
5.41	$[M-H]^-$	165.99691	167.00419		
3.43	$[M+H]^+$	168.01130	167.00403		
3.62	$[M+H]^+$	168.01128	167.00401		
4.19	$[M+H]^+$	168.01122	167.00395		
4.63	$[M+H]^+$	168.01125	167.00397		
4.92	$[M+H]^+$	168.01127	167.00399		
5.22	$[M+H]^+$	168.01127	167.00399		
5.47	$[M+H]^+$	168.01122	167.00394		
1.46	$[M+H]^+$	184.00614	182.99886	$C_7H_5NO_3S$	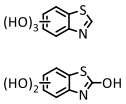
1.94	$[M+H]^+$	184.00613	182.99886		
2.33	$[M+H]^+$	184.00617	182.99890		
2.60	$[M+H]^+$	184.00613	182.99886		
3.12	$[M+H]^+$	184.00620	182.99893		
3.86	$[M+H]^+$	184.00616	182.99888		
4.04	$[M+H]^+$	184.00613	182.99886		
4.44	$[M+H]^+$	184.00615	182.99887		
1.69	$[M-H]^-$	213.98179	214.98906	$C_7H_5NO_5S$	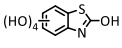
3.93	$[M-H]^-$	213.98177	214.98905		
4.56	$[M-H]^-$	213.98173	214.98900		
1.32	$[M+H]^+$	215.99622	214.98895		
1.61	$[M+H]^+$	215.99618	214.98891		
2.08	$[M+H]^+$	215.99618	214.98890		

Table S5. Proposed oligomers with the BT moiety from the BT-pH2 experiment analyzed by LC-Orbitrap MS.

Retention time (min)	Ion mode	m/z	Calc. MW	Formula	Proposed structure
6.25	$[M+H]^+$	269.02043	268.01315		
6.39	$[M+H]^+$	269.02038	268.01310		
6.95	$[M+H]^+$	269.02042	268.01315		
7.11	$[M+H]^+$	269.02048	268.01320	$C_{14}H_8N_2S_2$	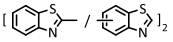
7.27	$[M+H]^+$	269.02042	268.01313		
7.59	$[M+H]^+$	269.02040	268.01312		
8.08	$[M+H]^+$	269.02036	268.01305		
5.83	$[M-H]^-$	283.00069	284.00796		
6.22	$[M-H]^-$	283.00075	284.00802		
6.34	$[M-H]^-$	283.00066	284.00793		
6.44	$[M-H]^-$	283.00067	284.00795		
6.76	$[M-H]^-$	283.00076	284.00804		
7.61	$[M-H]^-$	283.00072	284.00799		
5.67	$[M+H]^+$	285.01531	284.00803		
5.83	$[M+H]^+$	285.01534	284.00806		
6.23	$[M+H]^+$	285.01533	284.00806	$C_{14}H_8N_2OS_2$	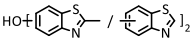
6.35	$[M+H]^+$	285.01532	284.00804		
6.44	$[M+H]^+$	285.01538	284.00810		
6.54	$[M+H]^+$	285.01523	284.00796		
6.76	$[M+H]^+$	285.01518	284.00791		
6.98	$[M+H]^+$	285.01534	284.00806		
7.18	$[M+H]^+$	285.01535	284.00807		
7.62	$[M+H]^+$	285.01524	284.00797		
8.57	$[M+H]^+$	285.01520	284.00792		
5.75	$[M-H]^-$	298.99562	300.00290		
6.03	$[M-H]^-$	298.99557	300.00285		
6.14	$[M-H]^-$	298.99558	300.00286		
6.79	$[M-H]^-$	298.99571	300.00299		
5.16	$[M+H]^+$	301.01009	300.00281		
5.48	$[M+H]^+$	301.01003	300.00275	$C_{14}H_8N_2O_2S_2$	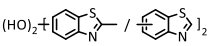
5.73	$[M+H]^+$	301.01015	300.00287		
5.90	$[M+H]^+$	301.01021	300.00294		
6.15	$[M+H]^+$	301.01011	300.00284		
6.67	$[M+H]^+$	301.01019	300.00292		
6.79	$[M+H]^+$	301.01009	300.00281		

5.02	$[M-H]^-$	314.99053	315.99780	$C_{14}H_8N_2O_3S_2$	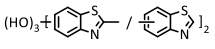
5.64	$[M-H]^-$	314.99052	315.99780		
5.01	$[M+H]^+$	317.00499	315.99771		
5.64	$[M+H]^+$	317.00516	315.99788		
4.86	$[M-H]^-$	330.98549	331.99277	$C_{14}H_8N_2O_4S_2$	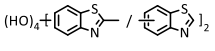
5.49	$[M-H]^-$	330.98550	331.99278		
5.71	$[M-H]^-$	330.98554	331.99281		
4.82	$[M+H]^+$	332.99993	331.99266		
4.30	$[M-H]^-$	346.98042	347.98770	$C_{14}H_8N_2O_5S_2$	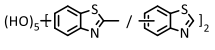
5.11	$[M-H]^-$	346.98041	347.98769		
5.17	$[M-H]^-$	346.98040	347.98768		
4.29	$[M+H]^+$	348.99492	347.98763		
4.47	$[M+H]^+$	348.99489	347.98761		
3.96	$[M-H]^-$	362.97546	363.98274	$C_{14}H_8N_2O_6S_2$	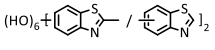
5.03	$[M-H]^-$	362.97523	363.98251		
3.21	$[M+H]^+$	364.98981	363.98252		
3.97	$[M+H]^+$	364.98969	363.98239		
5.22	$[M-H]^-$	378.97026	379.97754	$C_{14}H_8N_2O_7S_2$	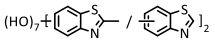
5.52	$[M+H]^+$	465.99832	464.99108	$C_{21}H_{11}N_3O_4S_3$	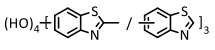

Table S6. Proposed ring-opening and fragmentation products from the BT-pH2 experiment analyzed by LC-Orbitrap MS.

Retention time (min)	Ion mode	m/z	Calc. MW	Formula	Proposed structure
2.15	$[M+H]^+$	170.02692	169.01964		
2.39	$[M+H]^+$	152.01636	169.01966		
2.89	$[M+H]^+$	170.02691	169.01963	$C_7H_7NO_2S$	
3.55	$[M+H]^+$	170.02692	169.01964		
4.10	$[M+H]^+$	170.02692	169.01964		
4.30	$[M+H]^+$	152.01636	169.01964		
4.37	$[M+H]^+$	126.03710	125.02983	C_6H_7NS	
4.73	$[M+H]^+$	126.03707	125.02980		
2.54	$[M-H]^-$	215.99739	217.00467		
2.86	$[M-H]^-$	215.99738	217.00466		
4.36	$[M-H]^-$	215.99733	217.00461		
1.32	$[M+H]^+$	218.01189	217.00462	$C_7H_7NO_5S$	
1.58	$[M+H]^+$	218.01179	217.00453		
1.81	$[M+H]^+$	218.01180	217.00452		
2.11	$[M+H]^+$	218.01183	217.00455		
2.55	$[M+H]^+$	218.01188	217.00460		
2.49	$[M-H]^-$	172.00739	173.01467		
1.81	$[M+H]^+$	174.02184	173.01457		
2.49	$[M+H]^+$	174.02183	173.01455	$C_6H_7NO_3S$	
3.99	$[M+H]^+$	174.02182	173.01454		
4.21	$[M+H]^+$	174.02181	173.01454		
4.22	$[M+H]^+$	154.04975	153.04247	$C_7H_7NO_3$	
4.84	$[M-H]^-$	108.04564	109.05292		
4.51	$[M+H]^+$	110.05995	109.05267	C_6H_7NO	
4.84	$[M+H]^+$	110.05992	109.05264		
4.72	$[M-H]^-$	109.02965	110.03692	$C_6H_6O_2$	
1.34	$[M+H]^+$	143.03377	142.02651	$C_6H_6O_4$	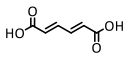
1.48	$[M+NH_4]^+$	118.04979	100.01596	$C_4H_4O_3$	
2.47	$[M+H]^+$	165.99561	164.98834		
3.48	$[M+H]^+$	165.99563	164.98835	$C_7H_3NO_2S$	
4.70	$[M+H]^+$	165.99559	164.98831		

1.32	$[M-H]^-$	231.99234	232.99962		
1.67	$[M-H]^-$	231.99232	232.99960		
2.50	$[M-H]^-$	231.99230	232.99958		
3.02	$[M-H]^-$	231.99236	232.99964	$C_7H_7NO_6S$	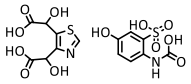
3.77	$[M-H]^-$	231.99237	232.99965		
1.71	$[M+H]^+$	234.00670	232.99943		
1.88	$[M+H]^+$	234.00673	232.99945		
2.25	$[M+H]^+$	234.00685	232.99956		
1.66	$[M-H]^-$	201.98177	202.98904		
2.05	$[M-H]^-$	201.98176	202.98903	$C_6H_5NO_5S$	
3.67	$[M-H]^-$	201.98174	202.98902		
1.31	$[M+H]^+$	203.99623	202.98895		
2.24	$[M-H]^-$	171.97100	172.97828		
1.32	$[M+H]^+$	173.98544	172.97816	$C_5H_3NO_4S$	
2.25	$[M+H]^+$	173.98544	172.97816		
1.51	$[M+H]^+$	202.01688	201.00960		
1.73	$[M+H]^+$	202.01693	201.00966		
1.92	$[M+H]^+$	202.01694	201.00966		
2.36	$[M+H]^+$	202.01696	201.00968	$C_7H_7NO_4S$	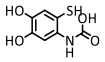
3.64	$[M+H]^+$	202.01698	201.00969		
4.13	$[M+H]^+$	202.01699	201.00971		
5.70	$[M+H]^+$	202.01701	201.00973		
1.32	$[M-H]^-$	265.99776	267.00504	$C_7H_9NO_8S$	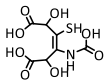
1.32	$[M-H]^-$	235.98721	236.99447	$C_6H_7NO_7S$	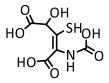
1.29	$[M+H-H_2O]^+$	219.99108	236.99439		
1.27	$[M-H]^-$	205.97657	206.98385	$C_5H_5NO_6S$	
4.65	$[M+H]^+$	142.03200	141.02472	C_6H_7NOS	
2.88	$[M+H]^+$	158.02689	157.01962		
3.23	$[M+H]^+$	158.02691	157.01964		
3.75	$[M+H]^+$	158.02692	157.01964	$C_6H_7NO_2S$	
4.07	$[M+H]^+$	158.02692	157.01964		
4.78	$[M+H]^+$	158.02692	157.01964		
1.33	$[M+H]^+$	156.01134	155.00403		
2.23	$[M+H]^+$	156.01126	155.00398		
2.58	$[M+H-H_2O]^+$	138.00072	155.00398	$C_6H_5NO_2S$	
2.81	$[M+H+MeOH]^+$	188.03745	155.00397		
3.33	$[M+H]^+$	156.01127	155.00399		

1.63	$[M+H]^+$	186.02177	185.01449		
1.81	$[M+H]^+$	186.02181	185.01454		
1.99	$[M+H]^+$	186.02184	185.01457		
2.72	$[M+H]^+$	186.02175	185.01448		
2.97	$[M+H]^+$	186.02180	185.01453	$C_7H_7NO_3S$	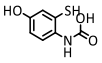
3.43	$[M+H]^+$	186.02187	185.01459		
3.76	$[M+H]^+$	186.02181	185.01454		
3.95	$[M+H]^+$	186.02178	185.01451		
4.19	$[M+H]^+$	186.02172	185.01445		
4.35	$[M+H]^+$	186.02182	185.01454		
6.11	$[M+H]^+$	285.98674	284.97945	$C_6H_7NO_{10}S$	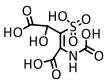
1.57	$[M+H]^+$	190.01668	189.00940		
1.99	$[M+H]^+$	190.01677	189.00950	$C_6H_7NO_4S$	
2.55	$[M+H]^+$	190.01672	189.00945		
1.64	$[M-H]^-$	203.99736	205.00463		
2.50	$[M-H]^-$	203.99732	205.00460	$C_6H_7NO_5S$	
2.13	$[M+H]^+$	206.01184	205.00456		
1.66	$[M-H]^-$	201.98177	202.98904		
2.05	$[M-H]^-$	201.98176	202.98903	$C_6H_5NO_5S$	
3.67	$[M-H]^-$	201.98174	202.98902		
1.31	$[M+H]^+$	203.99623	202.98895		
1.29	$[M-H]^-$	239.98211	240.98939	$C_5H_7NO_8S$	
2.76	$[M+H]^+$	170.04467	169.03739	$C_7H_7NO_4$	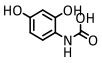
1.32	$[M+H]^+$	184.02387	183.01660	$C_7H_5NO_5$	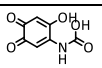
1.32	$[M+H]^+$	222.02447	221.01719	$C_6H_7NO_8$	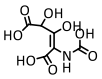
2.13	$[M+H]^+$	168.02903	167.02175	$C_7H_5NO_4$	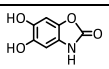
1.69	$[M+H]^+$	126.05485	125.04757		
3.10	$[M+H]^+$	126.05489	125.04761	$C_6H_7NO_2$	
4.22	$[M+H]^+$	126.05486	125.04758		
2.26	$[M+H]^+$	140.03413	139.02685	$C_6H_5NO_3$	
4.41	$[M+H]^+$	140.03411	139.02684		

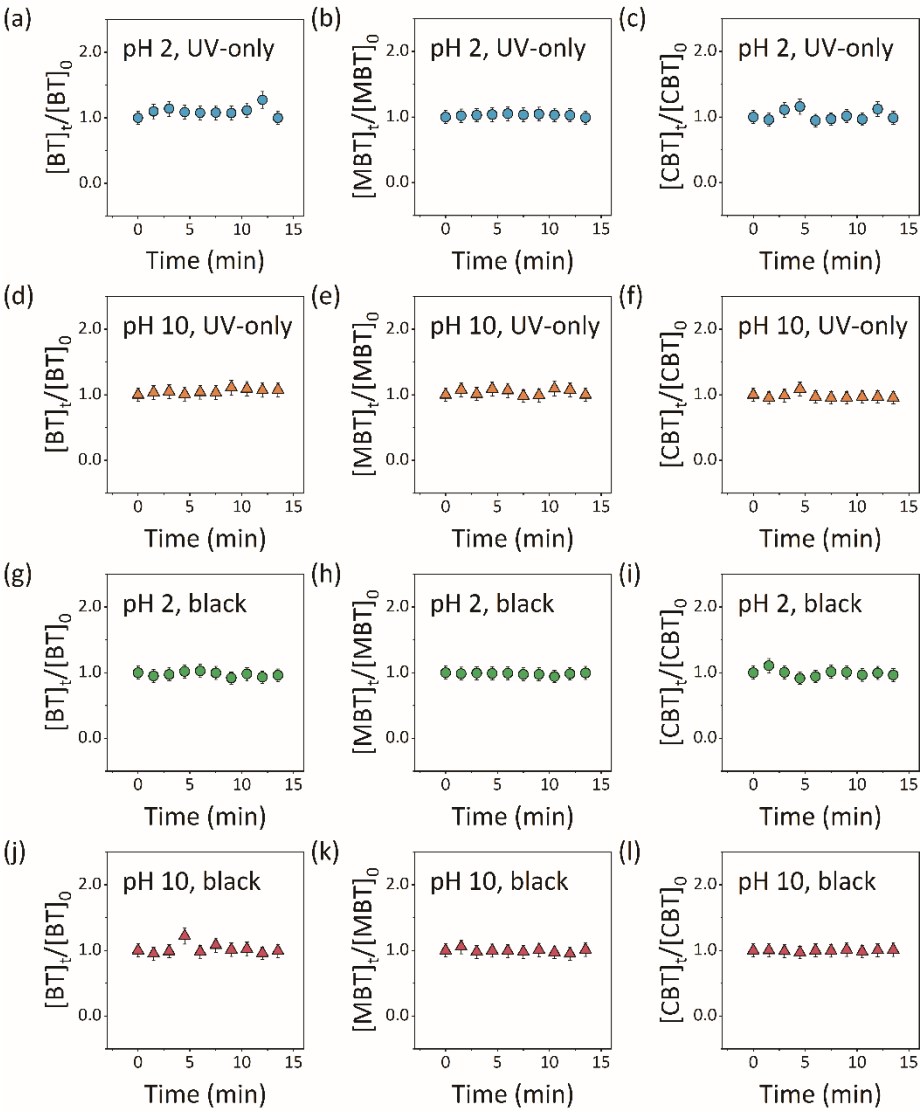

Figure S1. The ratio of intermediate time peak areas of BT, MBT, and CBT to their initial time peak areas (C_t/C_0) as a function of reaction time.

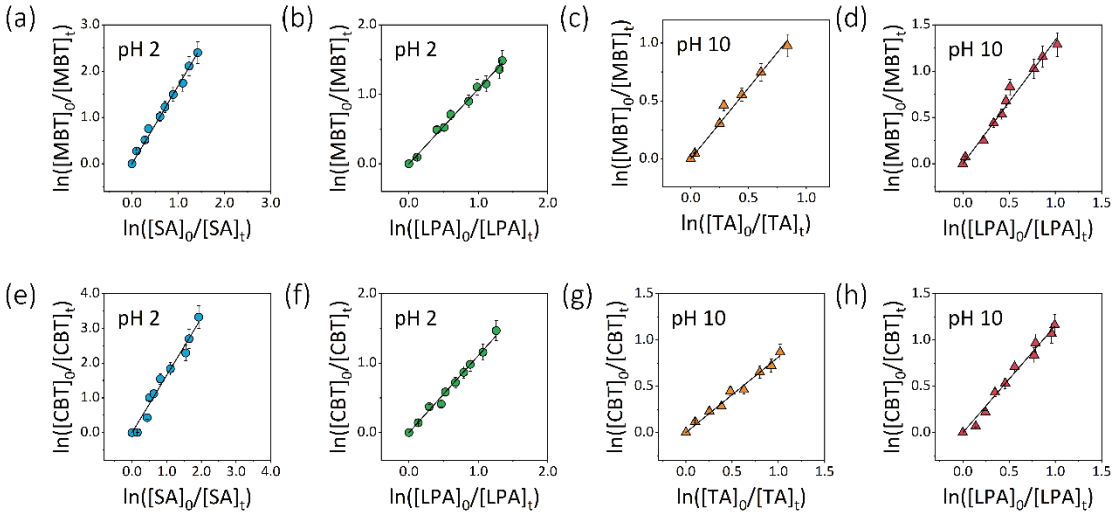

Figure S2. Relative kinetic plots for oxidation of MBT and CBT with OH radicals in the aqueous phase at initial pH 2 and 10 using SA, LPA, and TA as the reference compounds ($[BTs]_0$:$[Refs]_0$ = 1:1).

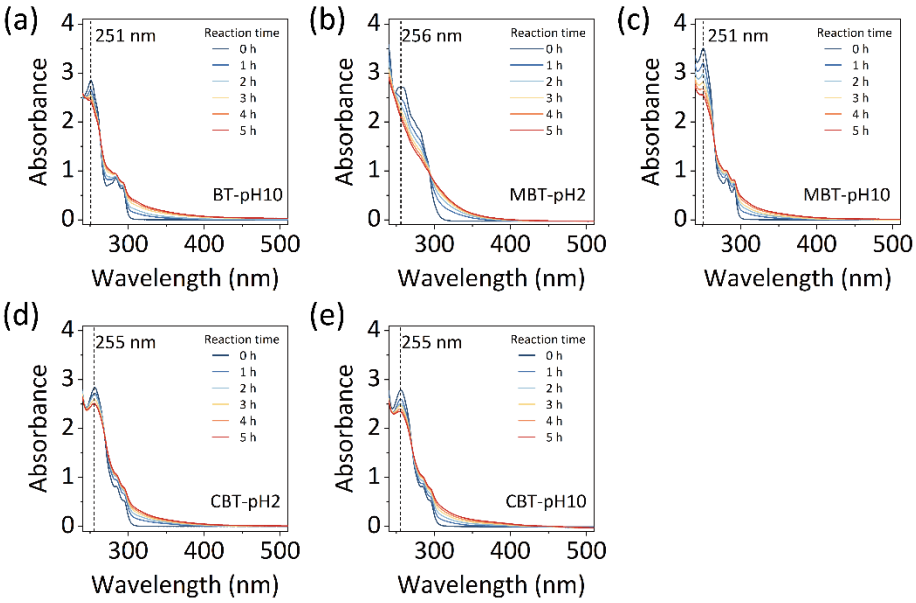

Figure S3. UV-vis absorption spectra of reaction solutions in Exps. BT-pH10 (a), MBT-pH2 (b), MBT-pH10 (c), CBT-pH2 (d), and CBT-pH10 (e) at reaction time intervals of 1 h.

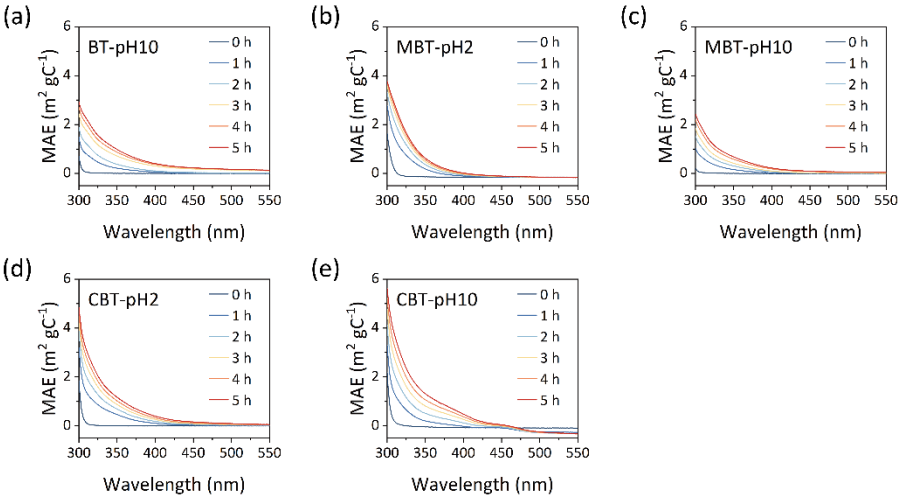

Figure S4. Mass absorption efficiency (MAE) of solutions in Exps. BT-pH10 (a), MBT-pH2 (b), MBT-pH10 (c), CBT-pH2 (d), and CBT-pH10 (e) at reaction time intervals of 1 h.

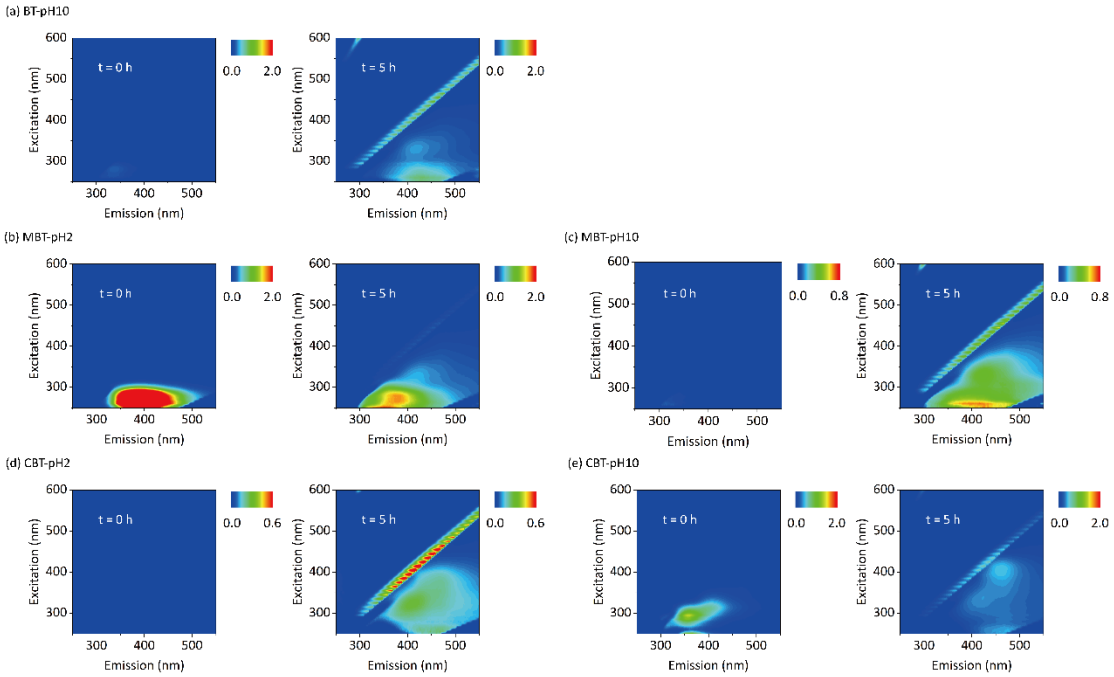

Figure S5. EEM fluorescence spectra of the reaction solution in Exps. BT-pH10 (a), MBT-pH2 (b), MBT-pH10 (c), CBT-pH2 (d), and CBT-pH10 (e) at reaction time 0 and 5 h.

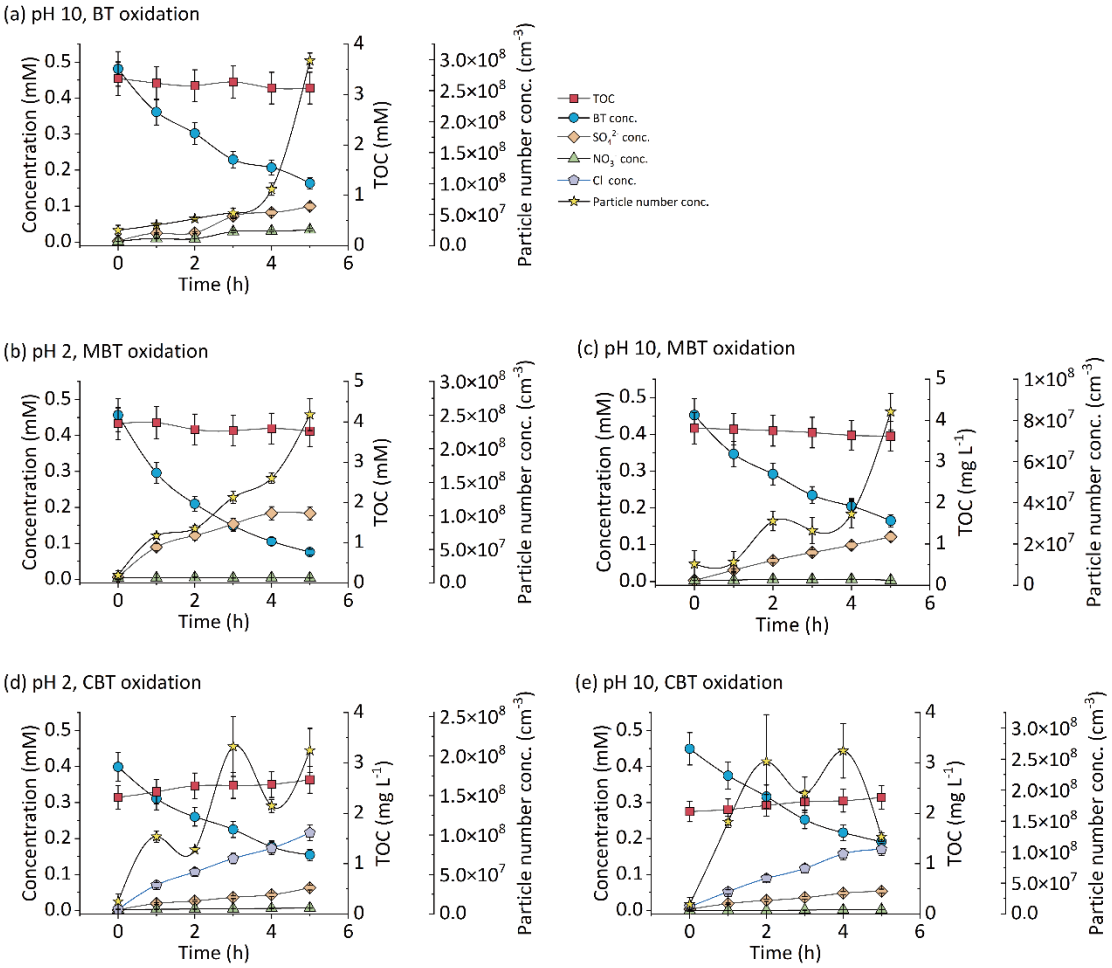

Figure S6. Time profiles of BT, MBT, and CBT degradation, inorganic products formation (SO_4^{2-}, NO_3^-, Cl^-), particles formation, and total organic carbon concentration in Exps. BT-pH10 (a), MBT-pH2 (b), MBT-pH10 (c), CBT-pH2 (d), and CBT-pH10 (e), respectively.

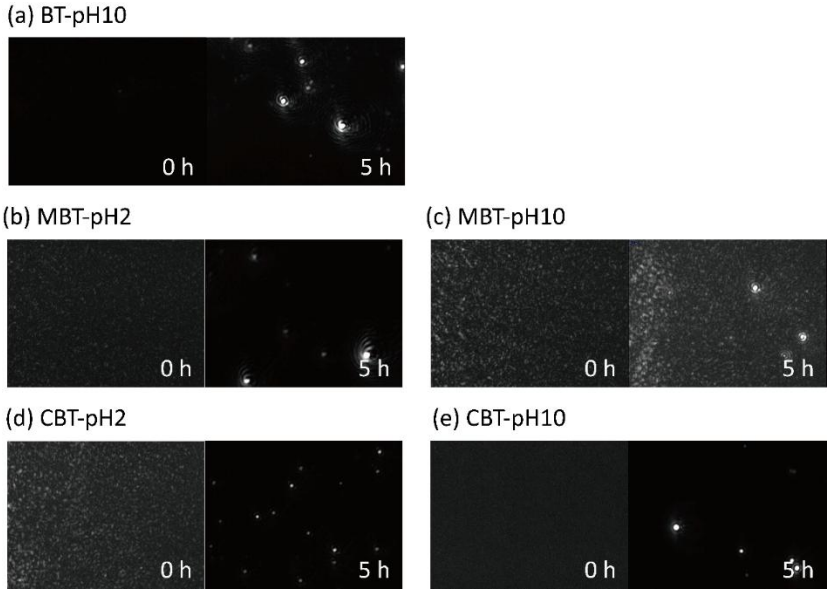

Figure S7. NTA images of samples collected before and after 5 hours of photooxidation in Exps. BT-pH10 (a), MBT-pH2 (b), MBT-pH10 (c), CBT-pH2 (d), and CBT-pH10 (e), respectively.

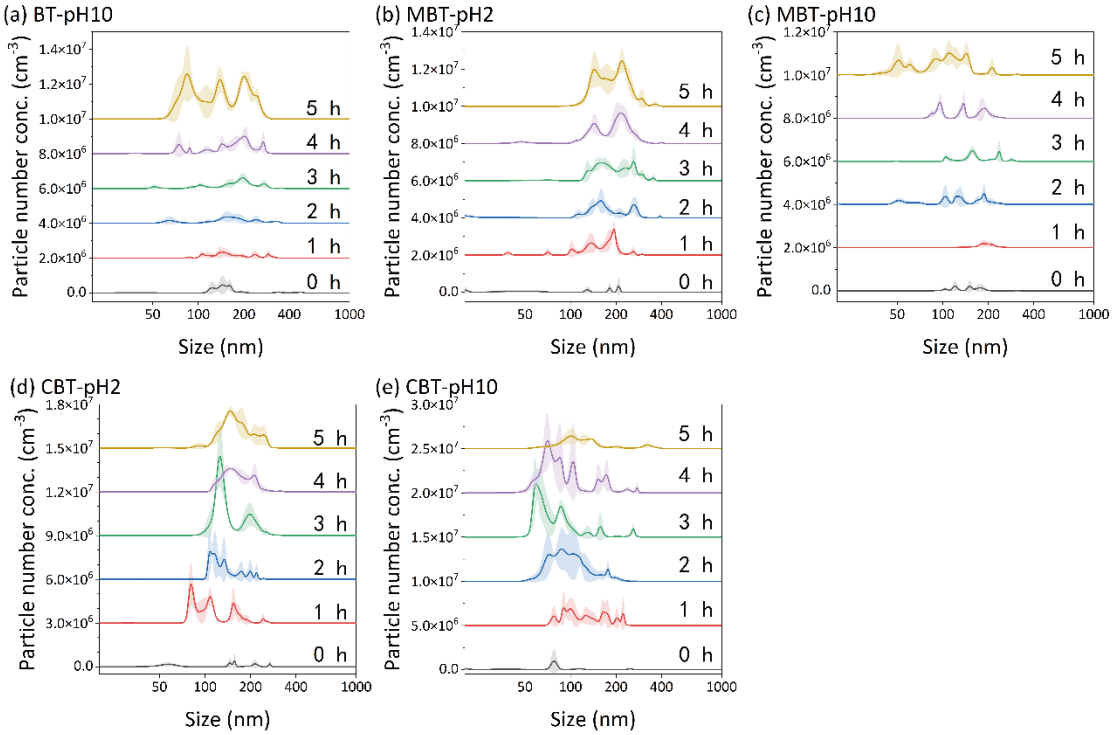

Figure S8. Size distribution of nanoparticles formed in Exps. BT-pH10 (a), MBT-pH2 (b), MBT-pH10 (c), CBT-pH2 (d), and CBT-pH10 (e) at reaction time intervals of 1 h.